OPEN ACCESS
CellPress

Cell Reports
Article

Phosphorylation and DNA Binding of HJURP Determine Its Centromeric Recruitment and Function in CenH3^{CENP-A} Loading

Sebastian Müller,[1,2,3,4,5] Rocio Montes de Oca,[1,2,3,4,5] Nicolas Lacoste,[1,2,3,4,5] Florent Dingli,[1,6] Damarys Loew,[1,6] and Geneviève Almouzni[1,2,3,4,5,*]
[1]Institut Curie, Centre de Recherche, Paris 75248, France
[2]CNRS, UMR3664, Paris 75248, France
[3]Equipe Labellisée Ligue contre le Cancer, UMR3664, Paris 75248, France
[4]UPMC, UMR3664, Paris 75248, France
[5]Sorbonne University, Paris 75005, France
[6]Laboratory of Proteomic Mass Spectrometry, 75248 Paris Cedex 05, France
*Correspondence: genevieve.almouzni@curie.fr
http://dx.doi.org/10.1016/j.celrep.2014.06.002
This is an open access article under the CC BY license (http://creativecommons.org/licenses/by/3.0/).

SUMMARY

Centromeres, epigenetically defined by the presence of the histone H3 variant CenH3, are essential for ensuring proper chromosome segregation. In mammals, centromeric CenH3^{CENP-A} deposition requires its dedicated chaperone HJURP and occurs during telophase/early G1. We find that the cell-cycle-dependent recruitment of HJURP to centromeres depends on its timely phosphorylation controlled via cyclin-dependent kinases. A nonphosphorylatable HJURP mutant localizes prematurely to centromeres in S and G2 phase. This unregulated targeting causes a premature loading of CenH3^{CENP-A} at centromeres, and cell-cycle delays ensue. Once recruited to centromeres, HJURP functions to promote CenH3^{CENP-A} deposition by a mechanism involving a unique DNA-binding domain. With our findings, we propose a model wherein (1) the phosphorylation state of HJURP controls its centromeric recruitment in a cell-cycle-dependent manner, and (2) HJURP binding to DNA is a mechanistic determinant in CenH3^{CENP-A} loading.

INTRODUCTION

The centromere is a specialized chromosomal domain usually defined by the primary constriction site on chromosomes (Flemming, 1882). During mitosis, it serves as the site for kinetochore assembly, a multiprotein complex that mediates spindle microtubule attachment (Cleveland et al., 2003). This specific organization ensures correct chromosome segregation and equal distribution of sister chromatids to both daughter cells during cell division. With the exception of budding yeast (Cheeseman et al., 2002), centromeres are not simply defined by an underlying DNA sequence but rather by chromatin features. This has led to consider centromeres as epigenetically defined chromosomal regions (reviewed in Allshire and Karpen, 2008; Probst et al., 2009). All eukaryotic centromeres are marked by a specific histone H3 variant (Black and Bassett, 2008; Fachinetti et al., 2013; Lacoste et al., 2014). Originally identified in mammals as CENP-A (Earnshaw and Rothfield, 1985), it has recently been called CenH3^{CENP-A}, using a nomenclature currently in discussion (Earnshaw et al., 2013; Earnshaw and Cleveland, 2013; Müller and Almouzni, 2014; Talbert et al., 2012; Talbert and Henikoff, 2013). Although this particular variant has been identified in many eukaryotic species, the timing of its incorporation differs between organisms (Allshire and Karpen, 2008; Boyarchuk et al., 2011). In *S. cerevisiae*, CenH3^{Cse4} incorporation occurs during DNA replication in S phase (Pearson et al., 2004), and in *S. pombe*, CenH3^{Cnp1} deposition takes place in early S phase and continues until G2 phase (Takayama et al., 2008). However, in mammalian cells, CenH3^{CENP-A} is diluted in S phase and distributed evenly to both daughter strands, and subsequently, its deposition is restricted to late telophase/early G1 (Jansen et al., 2007) (Figure 1A). A similar dilution in S phase is observed in *D. melanogaster*, but CenH3^{CID} assembly occurs between metaphase and anaphase as found in cultured fly cells (Mellone et al., 2011; Schuh et al., 2007). Much progress has been made concerning the understanding of the complex network of molecular players involved in the incorporation and maintenance of CenH3 at centromeres in different species (reviewed in Müller and Almouzni, 2014), but how they actually act at different times during the cell cycle remains elusive. The vertebrate CenH3^{CENP-A}-specific histone chaperone *H*olliday *ju*nction *r*ecognition *p*rotein (HJURP) (Dunleavy et al., 2009; Foltz et al., 2009), or its yeast homolog *s*uppressor of *c*hromosome *m*isse*g*regation protein *3* (Scm3) (Pidoux et al., 2009; Shivaraju et al., 2011), plays a central role for the proper incorporation of CenH3 into centromeric chromatin. In *D. melanogaster*, the protein *C*hromosome *al*ignment defect 1 (CAL1) is the dedicated CenH3^{CID} chaperone (Chen et al., 2014) but is not conserved with HJURP or Scm3. Notably, HJURP misregulation can lead to chromosome instability and mitotic defects (Dunleavy et al.,

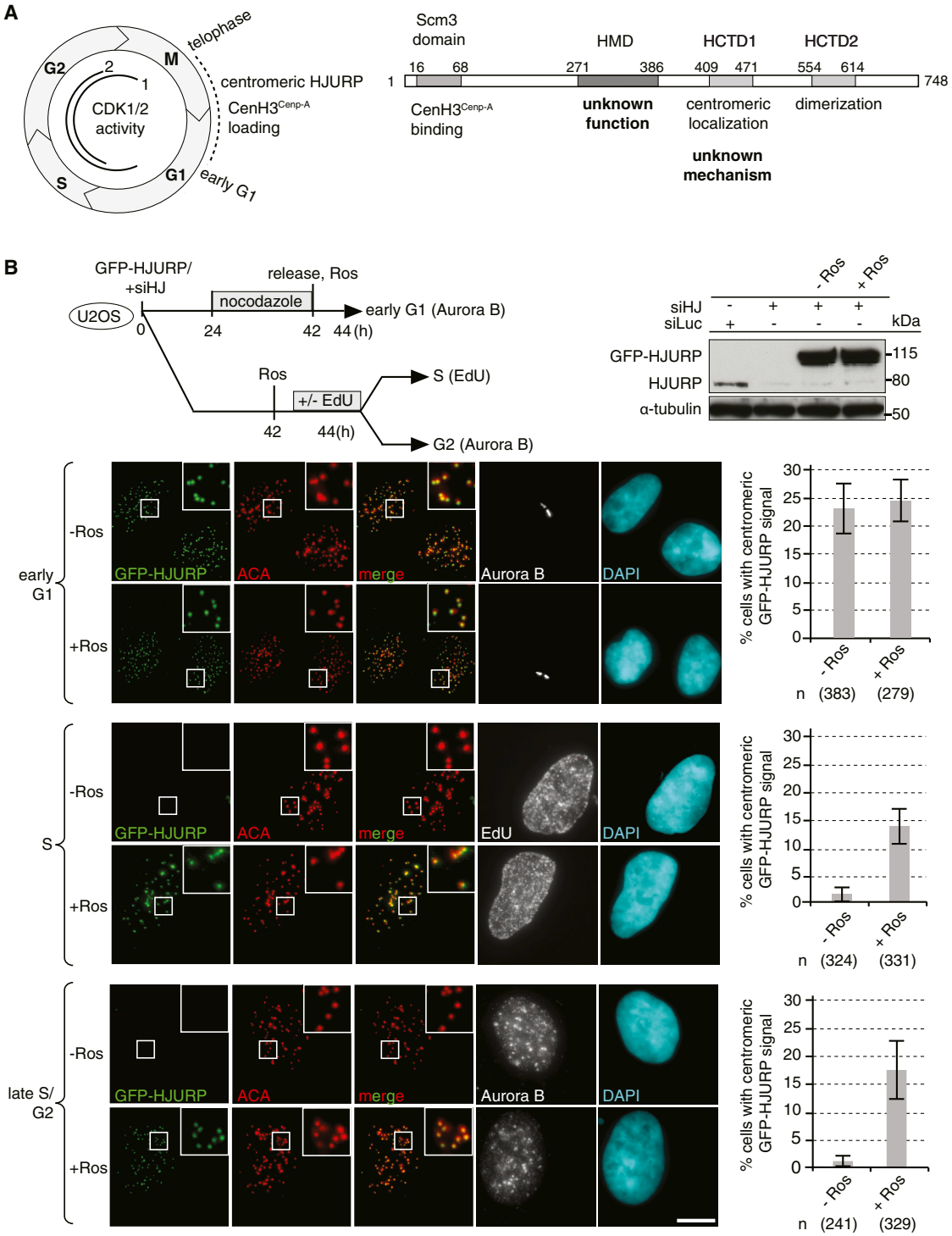

Figure 1. Centromeric Localization of HJURP Depends on CDK Activity

(A) Left: cell-cycle scheme and timing of centromeric HJURP localization/CenH3^{CENP-A} deposition. CDK1 and CDK2 activity is indicated. Right view shows HJURP and its domains with known and unknown functions.

(B) Top left: experimental scheme. Top-right view shows a western blot from U2OS cells expressing GFP-HJURP, transfected with siHJ or siLuc treated with or without Roscovitine (Ros). HJURP and GFP-HJURP are detected with a HJURP antibody. Bottom view shows images of cells expressing GFP-HJURP treated with or without Ros imaged in early G1, S, and G2. Scale bar, 5 μm. Percentages of cells with centromeric GFP signal in different cell-cycle phases are displayed on the right. Average of three independent experiments is shown. Error bars, SD.

See also Figure S1.

2009; Mishra et al., 2011). Its direct artificial targeting is sufficient to form a functional de novo kinetochore in human cells (Barnhart et al., 2011). Interestingly, overexpression of CenH3^{CENP-A} in cultured human cells leads to an enrichment at noncentromeric regions (Choi et al., 2011; Gascoigne et al., 2011). In this case, it is not HJURP but rather the H3.3 dedicated histone chaperone DAXX that is key for this ectopic localization (Lacoste et al., 2014). This is raising the issue of how HJURP can be specific for the targeting of CenH3^{CENP-A} strictly to centromeres, what is controlling the cell-cycle timing, and whether it has a mechanistic function to promote CenH3^{CENPA} loading.

In this respect, it is interesting to note that the cell-cycle timing of CenH3^{CENPA} loading is coupled to the activity of *c*yclin-*d*ependent *k*inase (CDK) 1 and 2, which phosphorylate Mis18BP (Silva et al., 2012). The latter is a subunit of the Mis18 complex (consisting of Mis18BP, Mis18α, and Mis18β), thought to prepare chromatin to be receptive for the loading of new CenH3^{CENP-A} (Fujita et al., 2007). CDK1 activity increases at the end of G1, peaks toward the end of G2/early M, and is reduced in anaphase, and CDK2 activity increases in mid-G1 and peaks in S/G2 (reviewed in Arellano and Moreno, 1997) (see Figure 1A). Interestingly, phosphorylation of HJURP and its ability to interact with DNA in vitro were discovered prior to its finding as a dedicated CenH3^{CENP-A} chaperone (Kato et al., 2007). Although early reports showed the involvement of the ATM kinase, more recent work showed that CDK1 can ensure a direct phosphorylation in vitro (Wang et al., 2014). Thus, which kinase can control HJURP phosphorylation in vivo remains unclear. However, more importantly, how such phosphorylation can contribute to HJURP function for a specific recruitment to centromeres specifically in telophase/early G1 has to be established. The recruitment of HJURP to centromeres is independent from its CenH3^{CENP-A}-binding domain (Zasadzińska et al., 2013); thus, the interaction with CenH3^{CENPA} to facilitate targeting can be excluded. Therefore, it is important to consider other domains of HJURP and whether their phosphorylation states depend on the cell cycle. The modular organization of HJURP reveals several key features. Its N-terminal histone-binding domain interacts with CenH3^{CENP-A} as a predeposition complex with histone H4 (Bassett et al., 2012; Hu et al., 2011; Shuaib et al., 2010). Whereas the N-terminal region of HJURP is conserved with yeast Scm3, a long C-terminal part is only found in vertebrates, which suggests functional differences between HJURP and Scm3. Indeed, vertebrate HJURPs are considerably larger than their Scm3 orthologs and contain three additional domains (Sanchez-Pulido et al., 2009). The HJURP C-terminal domain 1 (HCTD1) (409–471) is associated with centromeric targeting of HJURP, and the HCTD2 (554–614) is required for dimerization, which in turn is crucial for the loading of CenH3^{CENP-A} by HJURP at centromeres (Zasadzińska et al., 2013). Intriguingly, the function of the HJURP middomain (HMD) (271–386) is unknown (Figure 1A).

Here, we investigate how HJURP phosphorylation or its interaction with DNA contributes to its function as a CenH3^{CENP-A} chaperone. We consider an implication in (1) HJURP localization to centromeres and (2) its role in CenH3^{CENP-A} deposition, beyond a simple escort function to deliver CenH3^{CENP-A} to centromeres. Upon treatment with CDK inhibitors, we find that HJURP can be detected at centromeres in S and G2 phase. We map the phosphorylation state of the three critical residues Ser412, Ser448, and Ser473, which are inside or just adjacent to the HCTD1. A nonphosphorylatable HJURP mutant localizes to centromeres outside of telophase/early G1 and causes a premature loading of CenH3^{CENP-A} in G2, whereas a phosphomimic shows a reduction of centromeric localization in early G1 compared to the wild-type (WT). Furthermore, we identify a unique DNA-binding region in the HMD of HJURP that, surprisingly, proves dispensable for HJURP recruitment to centromeres. However, we find that this region is essential for the loading of CenH3^{CENP-A} at centromeres. Based on our findings, we propose a model in which (1) HJURP is recruited specifically in telophase/early G1 due to the dephosphorylation of its HCTD1 domain regulated by CDK activity, and (2) HJURP, through its DNA-binding domain, plays an essential role for CenH3^{CENP-A} loading, in addition to its CenH3^{CENP-A} escort function.

RESULTS

Cell-Cycle-Dependent Centromeric Localization of HJURP Is Controlled by CDK Activity

We postulated that CDKs directly control the localization of HJURP to centromeres in a cell-cycle-dependent manner (Figure 1A). To test this hypothesis, we investigated the effect of the kinase inhibitor Roscovitine on HJURP localization to centromeres in early G1, S, and G2 phase. Roscovitine strongly inhibits CDK1/CDK2 but also shows a broad spectrum of inhibition of other kinases. We used EdU or Aurora B as cell-cycle markers for S and G2, respectively, and human *a*nti*c*entromere *a*ntibody (ACA) as a centromeric marker (Figure S1A). Because HJURP can dimerize (Zasadzińska et al., 2013), the presence of endogenous HJURP may obscure phenotypic effects of exogenous protein. Thus, we downregulated endogenous HJURP using small interfering RNA (siRNA) against the 3′ UTR (siHJ), as evidenced by western blotting (Figure 1B). We found that treatment with Roscovitine did not impair localization of GFP-HJURP in early G1. However, GFP-HJURP localized to centromeres in S and G2 upon treatment with Roscovitine (Figure 1B). The presence of Roscovitine did not alter the expression levels of GFP-HJURP as shown by western blotting. As a positive control for the efficiency of Roscovitine treatment, we monitored the dephosphorylation of CAF-1 p60, which was previously reported to lose its phosphorylation as a result of Roscovitine treatment (Marheineke and Krude, 1998) (Figure S1B). We also tested another CDK1/CDK2 inhibitor, Purvalanol A. Both inhibitors did not alter the cell-cycle profile under the conditions used (Figure S1C). Treatment of cells with Purvalanol A also resulted in centromeric HJURP recruitment in S and G2 (Figure S1D). Taken together, this suggests that CDK activity regulates HJURP recruitment during the specific time window of late telophase/early G1 in a cell-cycle-dependent manner.

Phosphorylation of the HCTD1 Is Regulated in a Cell-Cycle-Dependent Manner

Next, we investigated whether the HJURP phosphorylation state changes at the M/G1 transition. For that, we synchronized U2OS cells with nocodazole and collected total cell extracts (1)

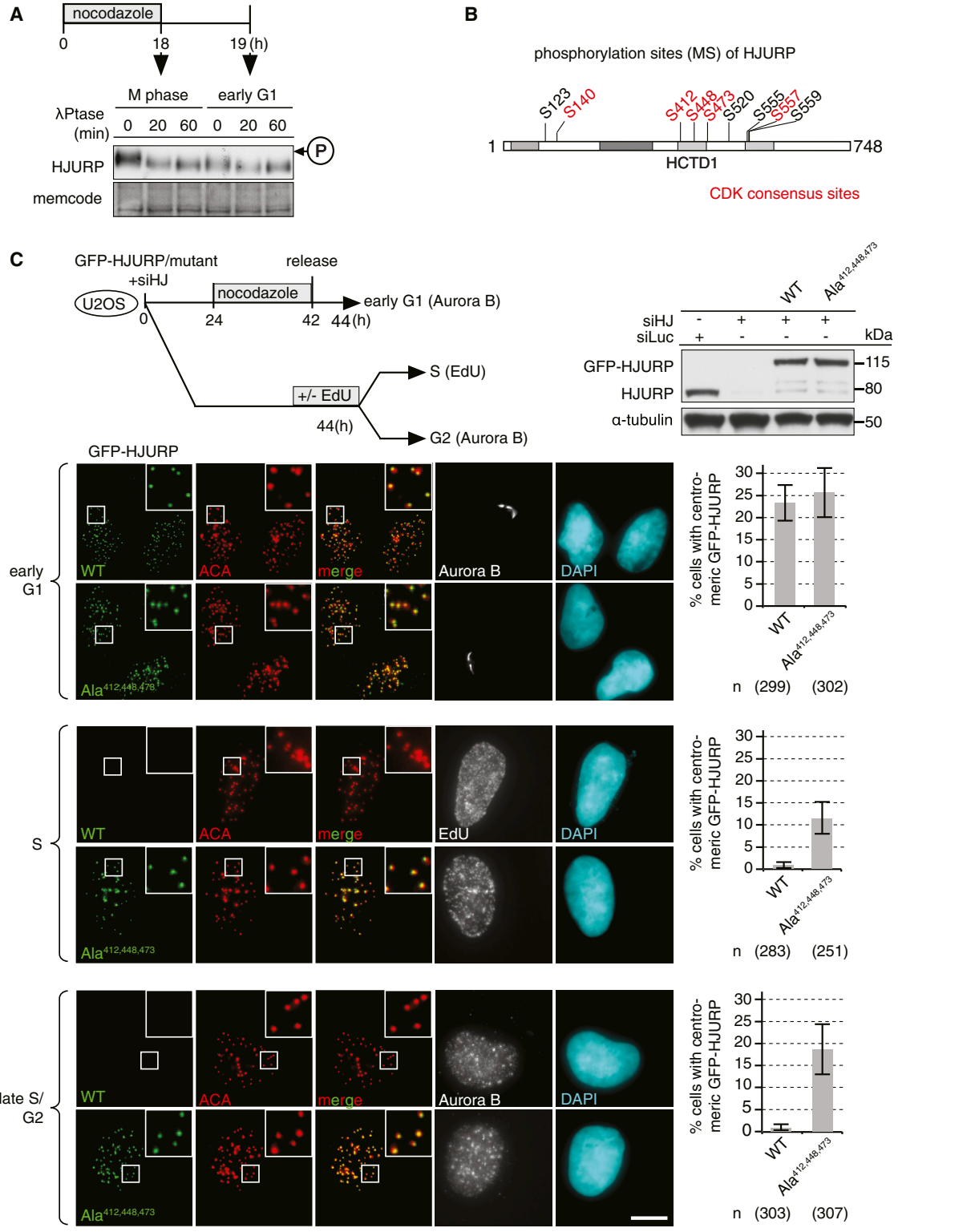

Figure 2. HJURP Phosphomutants Show Aberrant Cell-Cycle Localization to Centromeres in S and G2

(A) Experimental scheme and western blot showing a decrease of HJURP phosphorylation (circled "P") between M and early G1.

(B) Phosphorylation sites identified by MS. CDK consensus sites are highlighted in red.

(legend continued on next page)

directly after nocodazole release (M phase) and (2) 1 hr after release (early G1) and treated the extracts with λ phosphatase (Figure 2A). Nocodazole impairs microtubule polymerization and thus arrests cells in prometaphase. Upon nocodazole release, the cells pass through mitosis, and the population is enriched in G1 phase 1 hr after release (Figure S2A). A band shift in the western blot, indicative of HJURP phosphorylation, shows an increase in mitosis as compared to early G1 (Figure 2A). Treatment with λ phosphatase indicates that the higher band corresponds to hyperphosphorylated HJURP. This hyperphosphorylation in mitosis is lost upon entry into G1. Thus, a decrease in HJURP phosphorylation likely takes place at the end of mitosis. Next, we aimed to identify the phosphorylation sites of HJURP. For this, we transiently transfected U2OS cells with GFP-HJURP and pulled down the protein using the GFP-Trap system (Figure S2B). Subsequently, we isolated the corresponding band and searched for posttranslational modifications by mass spectrometry (MS). We found several phosphorylation sites, and some of these corresponded to CDK consensus sites (Dephoure et al., 2008), as depicted in Figure 2B. Three residues, which also correspond to CDK consensus sites (Ser412, Ser448, and Ser473) found inside or just adjacent to the HCTD1 (Figure S2C), attracted our attention. Indeed, this region proved to be important for HJURP localization to centromeres (Zasadzińska et al., 2013). We quantified the phosphorylation of the HCTD1 of GFP-HJURP isolated from M phase and G1 phase of the cell cycle by MS and found that phosphorylation decreased in G1 as compared to M phase. We also observed a decrease of phosphorylation of the HCTD1 in cells treated with Roscovitine (Figure S2D). Taken together, this suggests that Ser412, Ser448, and Ser473 are key residues of HJURP that undergo a decrease in phosphorylation at the M/G1 transition.

HJURP Phosphomutants Show Aberrant Cell-Cycle Localization at Centromeres

We then investigated the importance of these phosphorylation sites in the HCTD1 on centromeric HJURP localization. We generated distinct GFP-tagged mutants and studied their centromeric recruitment in a cell-cycle-dependent manner. In agreement with a previous report by Zasadzińska et al. (2013), the HCTD1 proved crucial for the recruitment of HJURP to centromeres (Figures S3A–S3C). Interestingly, our data also highlight that HJURP recruitment to centromeres is independent from its CenH3^{CENP-A}-binding domain.

Next, we generated a nonphosphorylatable triple mutant (Ala^{412,448,473}) by mutating the three serine residues in the HCTD1, which we had identified to be phosphorylated by MS, to alanine (Ala) (Figure 2B). We then studied the centromeric localization of this mutant throughout the cell cycle. We transiently transfected the WT GFP-HJURP or Ala^{412,448,473} into U2OS cells in the presence of siHJ. As expected, WT localized to centromeres in early G1, but not in S and G2 (Figure 2C). Ala^{412,448,473} also localized to centromeres in G1 in the same percentage of cells. Strikingly, in addition to G1, Ala^{412,448,473} was also recruited to centromeres in S and G2. We also generated the phosphomimic Glu^{412,448,473} to compare its centromeric localization throughout the cell cycle with WT and Ala^{412,448,473}. We cotransfected the constructs transiently in U2OS cells together with siHJ or siRNA against luciferase (siLuc) as a control. We verified by western blotting that both mutants and the WT construct expressed at similar levels, and siHJ downregulated endogenous HJURP but did not affect expression levels of the GFP-HJURP constructs (Figure S4A). We counted the cells with centromeric GFP signal of the WT and the mutants in the different cell-cycle phases (Figure S4A). Fewer cells recruited Glu^{412,448,473} in early G1 compared to WT and Ala^{412,448,473}, an effect that was enhanced upon treatment with siHJ. In S and G2, we observed more cells with centromere-positive Ala^{412,448,473} signal than for Glu^{412,448,473}. Finally, treatment with siHJ drastically increased the recruitment of Ala^{412,448,473} to centromeres in S and G2.

In order to dissect if these three residues act synergistically or if a single one is crucial for the observed aberrant cell-cycle localization of HJURP, we mutated these residues consecutively to Ala to generate the three single mutants Ala^{412}, Ala^{448}, and Ala^{473}. We found that all three single mutants localized to centromeres in G2, but this effect was more pronounced for the triple mutant Ala^{412,448,473} (Figure S4B). This suggests that cumulative dephosphorylation of all three residues facilitates HJURP localization to centromeres. Taken together with our observations with Roscovitine, we draw the following conclusions. First, dephosphorylation of the HCTD1, namely at Ser412, Ser448, and Ser473, leads to HJURP recruitment to centromeres in telophase/early G1. Second, phosphorylation favors HJURP dissociation from centromeres.

HJURP Interacts with DNA through a Single Conserved Domain Independently of CDK Activity

Given the previous characterization of HJURP as a DNA-interacting protein in vitro (Kato et al., 2007) and identification of an N-terminal DNA-binding region of Scm3 of *S. cerevisiae* (Xiao et al., 2011), we hypothesized that HJURP interaction with DNA could play a role in centromeric localization and/or the centromeric-loading mechanism of CenH3^{CENP-A}. First, we used a DNA-binding prediction software called DB-Bind (Hwang et al., 2007; Kuznetsov et al., 2006) to find putative DNA-binding regions of HJURP and Scm3 in various species (Figure 3A). With this method, in agreement with previous experimental data (Xiao et al., 2011), we verified the DNA-binding domain in the N-terminal region of Scm3 in *S. cerevisiae*. Interestingly, the Scm3 sequences of the different species showed no predicted conservation of the N-terminal DNA-binding region of *S. cerevisiae*. Surprisingly, in all the vertebrate species we investigated, this method predicted a DNA-binding region within the

(C) Top left: experimental scheme. Top-right view is a western blot showing expression levels of endogenous HJURP, GFP-HJURP, and GFP-Ala^{412,448,473} cotransfected with siLuc or siHJ, detected with a HJURP antibody. Bottom view shows images of cells expressing GFP-HJURP or GFP-Ala^{412,448,473} in the presence of siHJ imaged in G1, S, and G2. Scale bar, 5 μm. Percentages of cells with centromeric GFP signal in different cell-cycle phases are displayed on the right. Average of three independent experiments is shown. Error bar, SD.
See also Figures S2–S4.

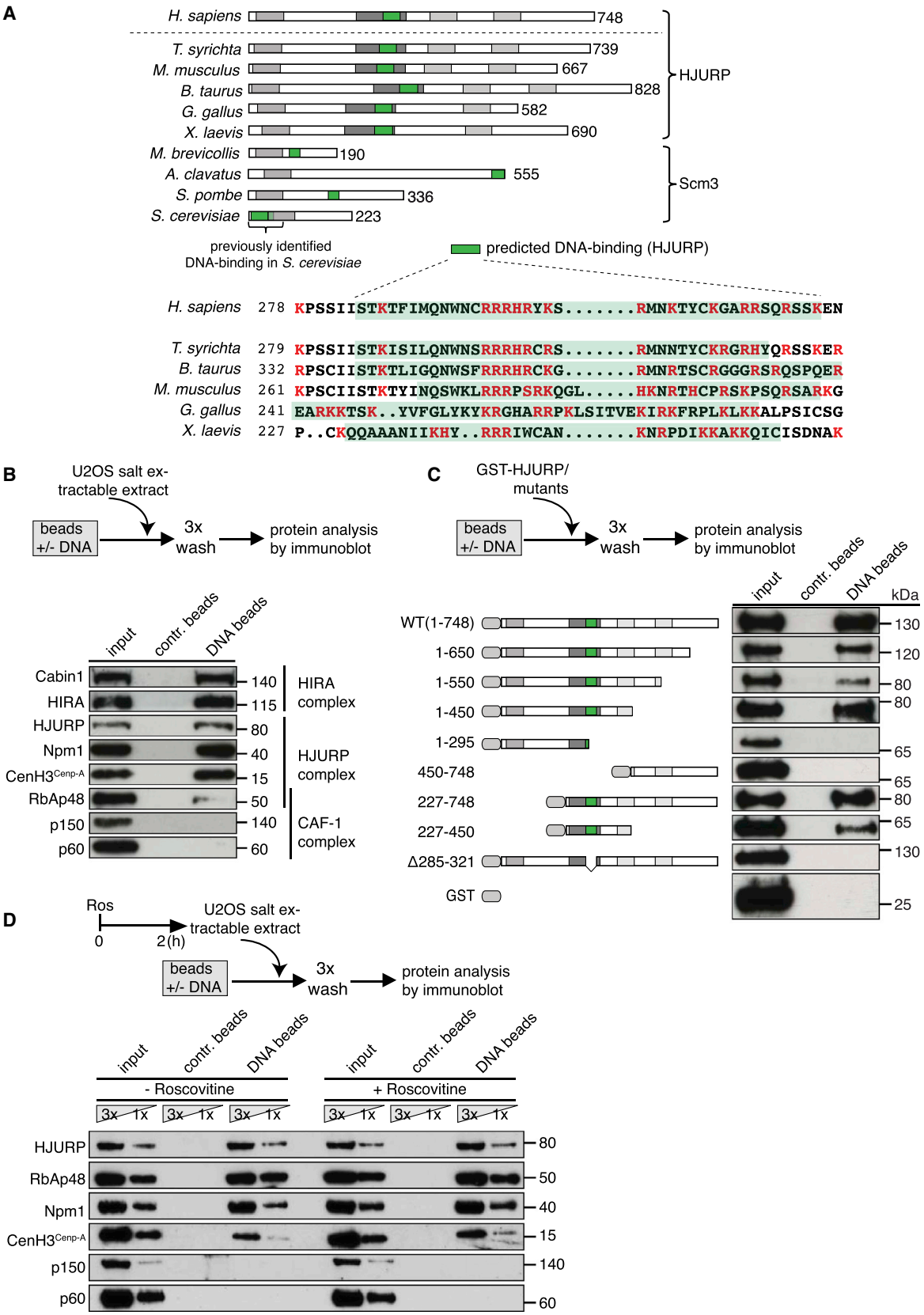

(legend on next page)

HMD of HJURP (Figures 3A, S5A, and S5B), and not in the CenH3^{CENP-A}-binding domain or the centromeric-targeting domain HCTD1. The presence of several basic amino acids in this region could in principle promote an interaction with the negatively charged backbone of DNA (Figure 3A).

Next, we used a DNA-binding assay, with DNA coupled to streptavidin magnetic beads (Mello et al., 2004; Ray-Gallet et al., 2011) and cell extracts. Using U2OS salt-extractable extracts (Martini et al., 1998), we looked at the retrieved proteins on the DNA beads including the HJURP complex, i.e., HJURP, Npm1, RbAp48, and CenH3^{CENP-A} (Dunleavy et al., 2009; Shuaib et al., 2010). We did not detect any signal with our control beads (Figure 3B). The presence of the histone H3.3 chaperone complex HIRA served as a positive control, whereas the histone H3.1 histone chaperone complex CAF-1 served as a negative control, consistent with our previous work (Ray-Gallet et al., 2011). Because the interaction in the extract can be indirect, it was important to test if HJURP interacts directly with DNA using recombinant protein. We thus produced glutathione S-transferase (GST)-HJURP and several mutants (Figures 3C and S5C) and tested these purified recombinant proteins for DNA interaction in the binding assay. We found that full-length HJURP interacts with DNA and that deleting the predicted DNA-binding region (285–321) abrogated its ability to bind DNA. Notably, the CenH3^{CENP-A}-binding domain and the HCTD1, important for centromeric localization of HJURP, proved dispensable for DNA binding (Figure 3C). Because the sequence of the HMD is not conserved with other DNA-binding proteins (Sanchez-Pulido et al., 2009), this may constitute a new type of DNA-binding domain.

We then investigated if CDK activity influences the binding of HJURP to DNA. We thus used extracts from cells treated with or without Roscovitine in the DNA-binding assay. We found that there was no difference in DNA binding (Figure 3D). Thus, CDK activity does not control the binding activity of HJURP to DNA as assayed in our experiments. These data suggest that HJURP is able to directly interact with DNA through a conserved DNA-binding domain in the HMD, independently of CDK activity.

De Novo Deposition of CenH3^{CENP-A} in Early G1 Requires DNA Binding of HJURP

We next explored the role of the DNA-binding domain in the centromeric CenH3^{CENP-A}-loading mechanism. For this, we used a U2OS cell line stably expressing SNAP-CenH3^{CENP-A} (described in Dunleavy et al., 2011) (Figure S6A). The SNAP-tag technology allows fluorescent labeling of newly synthesized proteins to distinguish them from the total protein pool. This method allows to study the de novo deposition of CenH3^{CENP-A} at centromeres (Jansen et al., 2007). After quenching old SNAP-CenH3^{CENP-A} protein with O^6-benzylguanine (Q), the chase (C) period allows new protein synthesis, and a pulse (P) of tetramethylrhodamine (TMR) ensures the labeling of de novo-deposited SNAP-CenH3^{CENP-A} (QCP assay). Concomitantly, we synchronized cells with nocodazole and released them into early G1, as shown in Figure 4A. Downregulation of endogenous HJURP caused a reduction of the signal of de novo-incorporated CenH3^{CENP-A} to 38% upon treatment with siHJ compared to the control treated with siLuc (Figure 4A).

To study the effects of HJURP mutants on the loading of CenH3^{CENP-A}, we transiently transfected the GFP-HJURP (WT), a phosphomutant (Ala^{412,448,473}), a DNA-binding mutant (Δ285–321), and a mutant unable to bind CenH3^{CENP-A} (Δ14–41), together with siHJ into SNAP-CenH3^{CENP-A} U2OS cells (see scheme on Figure 4A). By western blot, we verified that expression of all constructs was at comparable levels and downregulation of endogenous HJURP effective by siHJ (Figure 4A). Addition of WT could rescue the signal to 88%. As expected, Δ14–41 could not rescue the signal because it cannot interact with CenH3^{CENP-A} to escort it to centromeres. Interestingly, Ala^{412,448,473} could fully rescue loading of CenH3^{CENP-A}, whereas Δ285–321 could not. From these experiments, we draw two main conclusions. First, dephosphorylation of the HCTD1 does not impair the ability of HJURP to deposit CenH3^{CENP-A}. Second, the DNA-binding region is necessary for HJURP to load CenH3^{CENP-A} onto centromeres in early G1. These data support the view in which HJURP, in addition to its CenH3^{CENP-A}-escorting function, displays another important role in the loading mechanism of CenH3^{CENP-A} within centromeric chromatin.

Ala^{412,448,473} and Δ285–321 Have Different Effects on Cell Cycle and Toxicity

It was then important to evaluate if the phosphomutant Ala^{412,448,473} and the DNA-binding mutant Δ285–321 have an effect on the cell cycle and on cell proliferation. We expressed GFP-HJURP and the mutants in U2OS cells and analyzed the cell-cycle profile by fluorescence-activated cell sorting (FACS) 72 hr posttransfection. We verified by western blotting that expression of all constructs was comparable (Figure 4B). We found that Ala^{412,448,473}, but not Δ285–321, causes a cell-cycle delay. Ala^{412,448,473} expression leads to an increase (18.6%–25.9%) of cells in G2 and an increase in S (35.4%–40.1%) as compared to the WT (Figures 4B and S5D). In contrast, the cell-cycle profile of cells expressing Δ285–321 was comparable to cells expressing the WT. Endogenous HJURP is still present

Figure 3. HJURP Has a DNA-Binding Domain in the HMD

(A) Prediction of DNA-binding sites of HJURP and Scm3 in various species. Bottom view shows a sequence alignment of predicted DNA-binding regions in selected vertebrate species. Basic amino acids are in red.

(B) Experimental scheme and western blot of the DNA-binding assay. Input corresponds to 33% of extract used for the experiment.

(C) GST constructs of HJURP and truncation mutants and western blot of the DNA-binding assay using recombinant GST-HJURP and mutants detected by a GST antibody. Input corresponds to 33% recombinant protein used for the experiment.

(D) Experimental scheme and western blot of the DNA-binding assay using salt-extractable extracts from U2OS cells treated with and without Ros. Input corresponds to 33% of extract used for the experiment.

See also Figure S5.

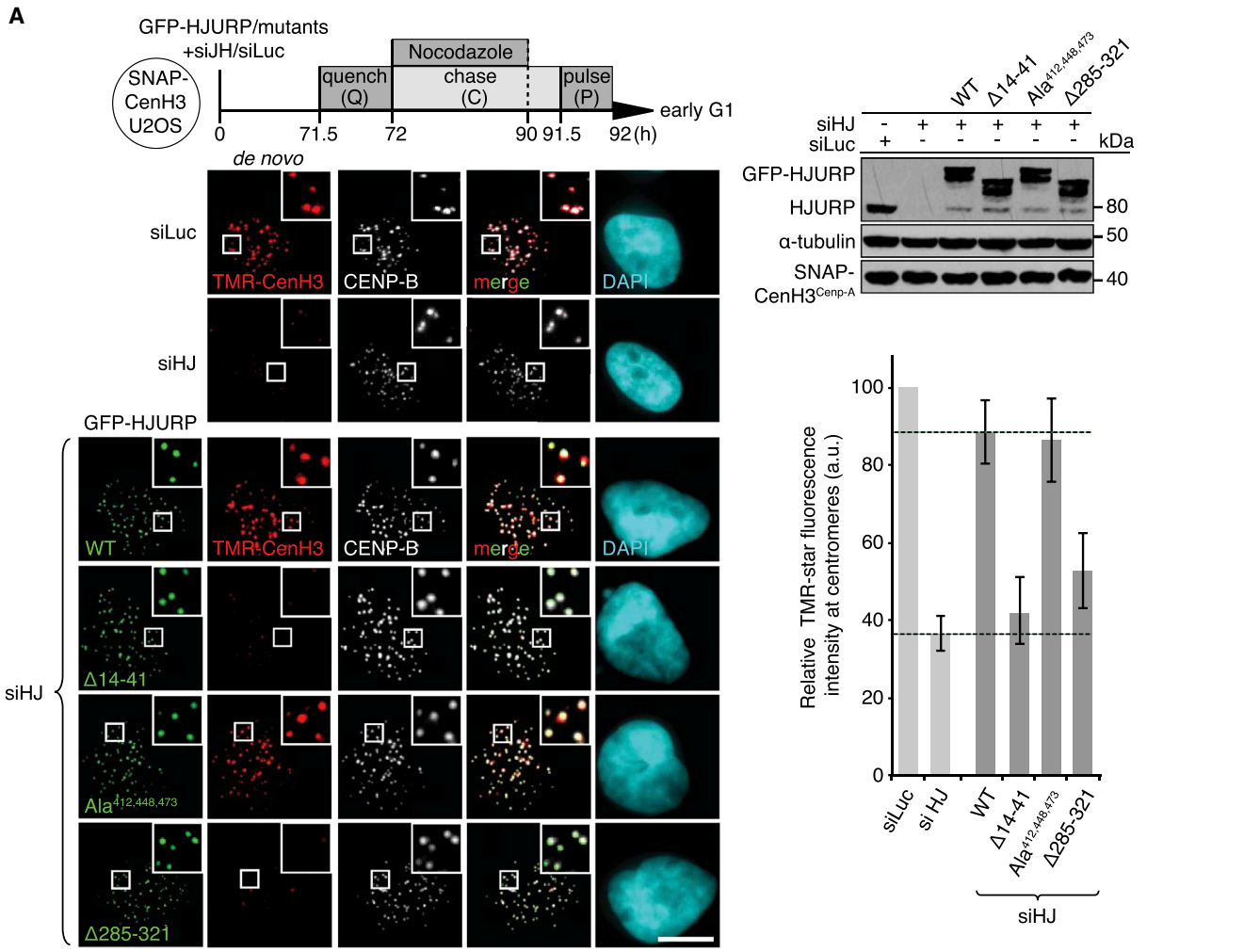

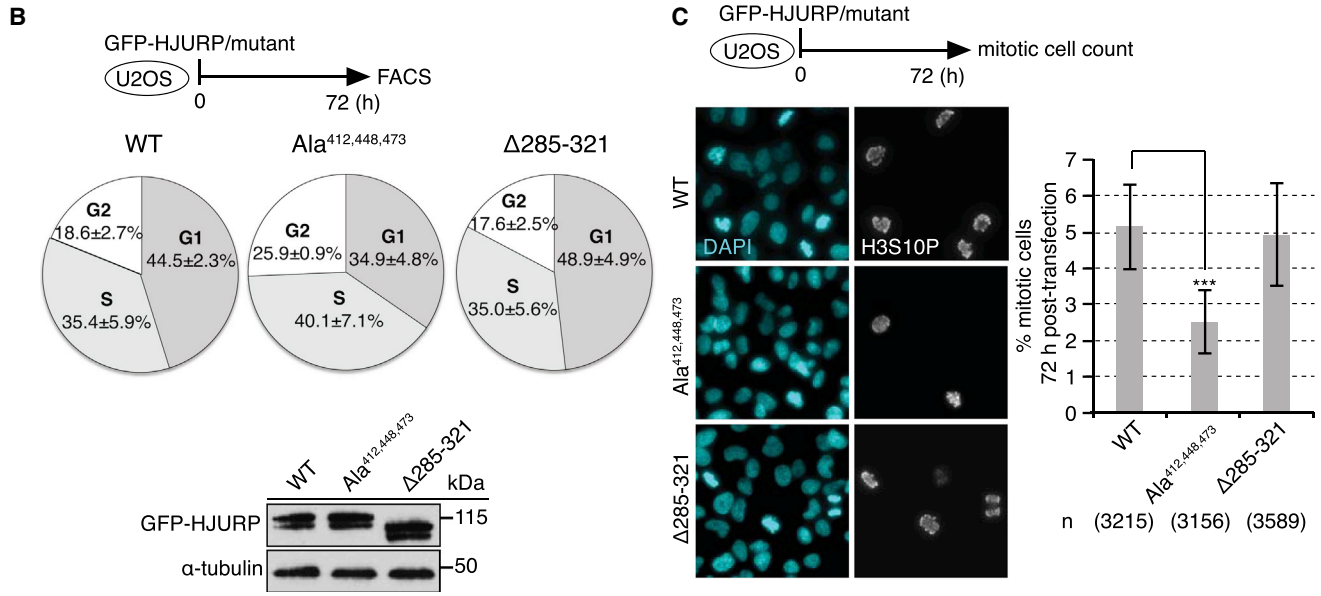

(legend on next page)

and can thus deposit CenH3^{CENP-A} in telophase/early G1, both in the presence of Δ285–321 and Ala^{412,448,474}. We counted mitotic cells 72 hr posttransfection using H3S10P as a marker, and whereas cells expressing WT or Δ285–321 showed a similar mitotic index, it was decreased in cells transfected with Ala^{412,448,473} (Figure 4C). Trypan blue exclusion 72 hr posttransfection (Figure S6B) showed no difference in viability between WT and Ala^{412,448,473}-treated cells but a decrease in viability caused by Δ285–321. Using a colony formation assay, we assessed long-term proliferation by counting colonies 12 days posttransfection. We observed a decrease in colony number for Ala^{412,448,473} and Δ285–321, which was more pronounced for the latter (Figure S6C). Taken together, different mechanistic aspects of HJURP likely impair long-term proliferation as judged in this assay. Whereas the DNA-binding mutant is immediately toxic to the cell because it cannot load CenH3^{CENP-A}, the nonphosphorylatable mutant causes cell-cycle delays, potentially mediated by its aberrant localization throughout the cell cycle.

Ala^{412,448,473} Loads CenH3^{CENP-A} at Centromeres in G2

We aimed to address whether the nonphosphorylatable mutant Ala^{412,448,473} could load CenH3^{CENP-A} in S and/or G2. First, we assessed if HJURP is involved in the aberrant loading of CenH3^{CENP-A} in S and G2 upon Roscovitine treatment (Silva et al., 2012). We synchronized SNAP-CenH3^{CENP-A} U2OS cells using a single thymidine block and released them after 3 hr (enriched in mid-S) or 8 hr (enriched in G2) (Figure S6D). We transfected cells either with siHJ or siLuc and treated them with Roscovitine. We saw a reduction of relative TMR fluorescence at centromeres in cells treated with siHJ as compared to cells treated with siLuc, both in S and G2 (Figure 5A). Cells were selected based on Aurora B or EDU staining typical for these cell-cycle phases. We observed a similar effect upon treatment with Purvalanol A (Figure S6E) and controlled the downregulation of endogenous HJURP by western blotting (Figure 5A). Taken together, we conclude that HJURP is the dedicated CenH3^{CENP-A} chaperone involved in the aberrant loading of CenH3^{CENP-A} at centromeres in S and G2 upon treatment with CDK inhibitors.

Next, we explored if the HJURP triple mutant Ala^{412,448,473} can deposit CenH3^{CENP-A} in S and/or G2. We transfected Ala^{412,448,473} and synchronized cells using a thymidine block and released them after 3, 6, or 8 hr to enrich cells in mid-S, late S, or G2, respectively (Figure S6D). We counted TMR-positive cells in mid-S, late S, and G2, selected by Aurora B or EDU staining typical for these cell-cycle phases. Strikingly, we found TMR-positive cells in 26% of Ala^{412,448,473}-positive cells in G2 but hardly any in mid-S or late S (Figure 5B). We also compared the number of TMR-CenH3^{CENP-A}-positive cells in mid-S, late S, and G2 between cells transfected with WT and Ala^{412,448,473} and only found a loading of CenH3^{CENP-A} in G2 with the Ala^{412,448,473} mutant, but not with the WT (Figures S6D–S6G). Taken together, this suggests that Ala^{412,448,473} can load CenH3^{CENP-A} in a subset of cells in G2, but not in S. This premature loading of CenH3^{CENP-A} by Ala^{412,448,473} could lead to the changes in the cell-cycle profile we had observed. This supports a view in which the timely loading of CenH3^{CENP-A} specifically in telophase/G1 is important for the correct functioning of the centromere in mammalian cells.

DISCUSSION

The CenH3^{CENP-A} chaperone HJURP plays a major role in centromere maintenance through its escort function for CenH3^{CENP-A}. It is a highly divergent protein with four distinct domains: the Scm3 domain, the HMD, the HCTD1, and the HCTD2 (Sanchez-Pulido et al., 2009). We found that the phosphorylation state of the HCTD1 is coupled to CDK activity and thus determines the recruitment of HJURP to centromeres specifically in telophase/early G1 (Figures 1 and 2). We also discovered that the HMD harbors a DNA-binding domain (Figure 3), which plays a role in the loading of CenH3^{CENP-A} at centromeres (Figure 4). Premature recruitment of a nonphosphorylatable HJURP mutant to centromeres leads to CenH3^{CENP-A} deposition in G2 (Figure 5). Thus, we assign additional functionalities to two domains of HJURP: the HMD and the HCTD1.

Our model is presented in Figure 6. Whereas the phosphorylation state of the HCTD1 determines the cell-cycle-dependent recruitment of HJURP to centromeres, the DNA-binding region of the HMD is necessary for CenH3^{CENP-A} loading by HJURP, assigning another function to HJURP in addition to its escorting role of CenH3^{CENP-A}. Our findings lead us to propose a three-step mechanism of the chaperone function of HJURP for CenH3^{CENP-A}, as depicted in Figure 6B. In step 1, HJURP is phosphorylated at the HCTD1 during most of the cell cycle and dephosphorylated at late stages of mitosis, concomitant with CDK1/CDK2 downregulation. This dephosphorylation causes a recruitment of HJURP to centromeres in telophase. In step 2, HJURP has a role in the loading process of CenH3^{CENP-A} at centromeres, where it functions mechanistically through a direct

Figure 4. De Novo CenH3^{CENP-A} Deposition Requires HJURP DNA Binding

(A) Top: experimental scheme and western blot showing the expression of the GFP constructs and downregulation of endogenous HJURP, both detected with a HJURP antibody. Bottom view shows images of SNAP-CenH3^{CENP-A} U2OS cells treated with siHJ or siLuc from rescue experiments with GFP-HJURP or the mutants: Δ14–41, Ala^{412,448,473}, and Δ285–321, cotransfected with siHJ. TMR-CenH3 corresponds to newly incorporated CenH3^{CENP-A} at centromeres. Centromeric localization is evidenced by colocalization with CENP-B. Scale bar, 5 μm. The bar chart represents the quantification of the fluorescent intensity of centromeric TMR-CenH3^{CENP-A} signal. The dashed lines represent the reduction in TMR signal upon siHJ treatment and the rescue measured with WT GFP-HJURP. Average of three independent experiments is shown. Error bars, SD.

(B) Experimental scheme and distribution in cell-cycle phases of cells transfected with WT GFP-HJURP or Ala^{412,448,473} or Δ285–321 72 hr posttransfection. Distribution of cell-cycle phases of cells treated with the different HJURP constructs is indicted. Average of three independent experiments is shown. The western blot shows comparable expression levels of all constructs.

(C) Experimental scheme and mitotic index of cells transfected with the GFP constructs: WT, Ala^{412,448,473}, or Δ285–321 at 72 hr posttransfection. Mitotic cells were revealed with a H3S10P antibody. Average of three independent experiments with one blind count is shown. Error bars, SD. ***$p < 0.001$ (Student's t test.). See also Figure S6.

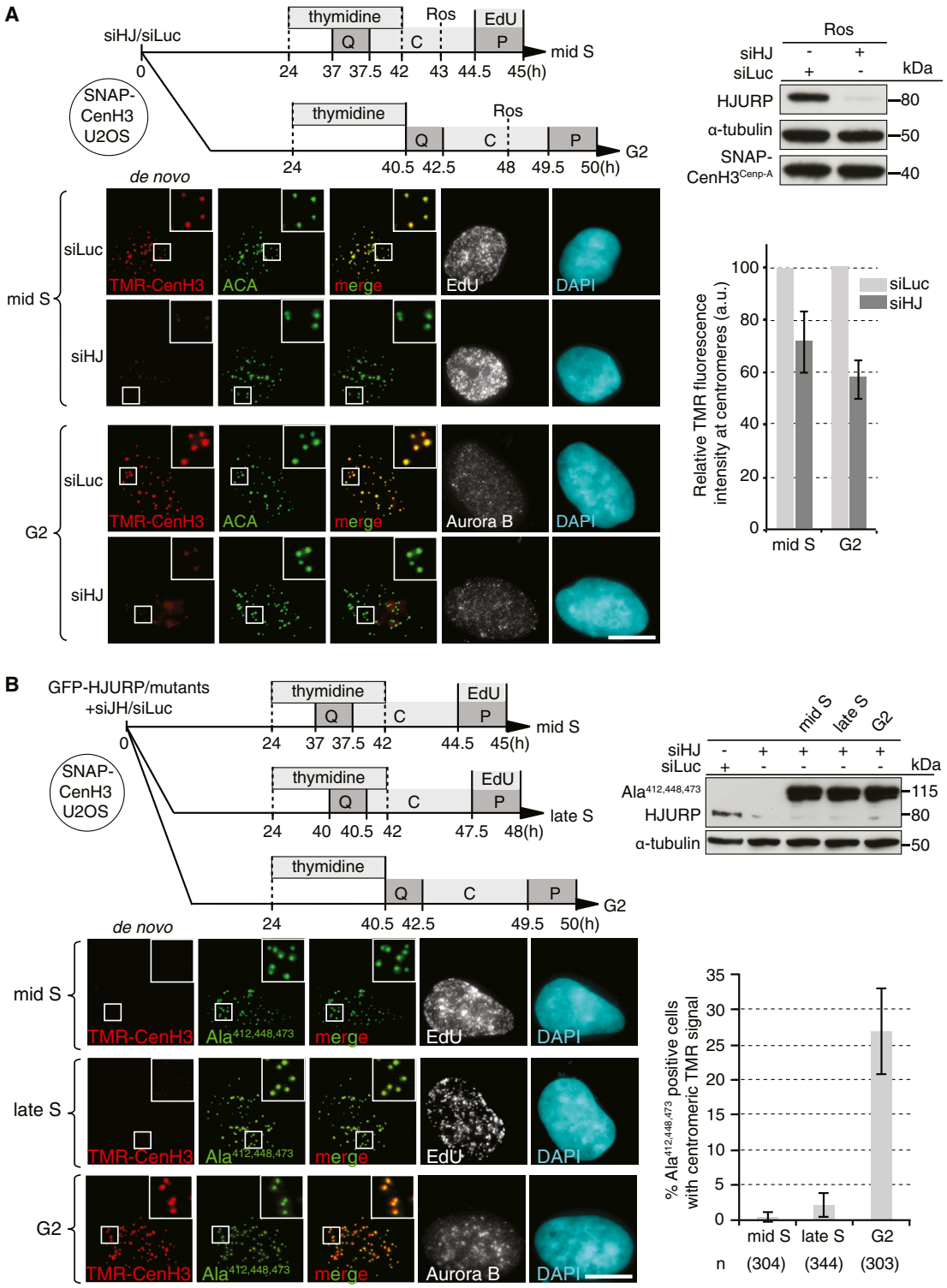

Figure 5. Ala^{412,448,473} Loads CenH3^{CENP-A} in G2

(A) Top: experimental schemes and western blot showing the expression of endogenous HJURP in the presence of siLuc or siHJ. Bottom view shows images of SNAP-CenH3^{CENP-A} U2OS cells transfected with siHJ or siLuc in S and G2 after treatment with Ros. Scale bar, 5 μm. The bar chart represents the quantification of the fluorescent intensity of TMR-CenH3^{CENP-A} signal at centromeres.

(legend continued on next page)

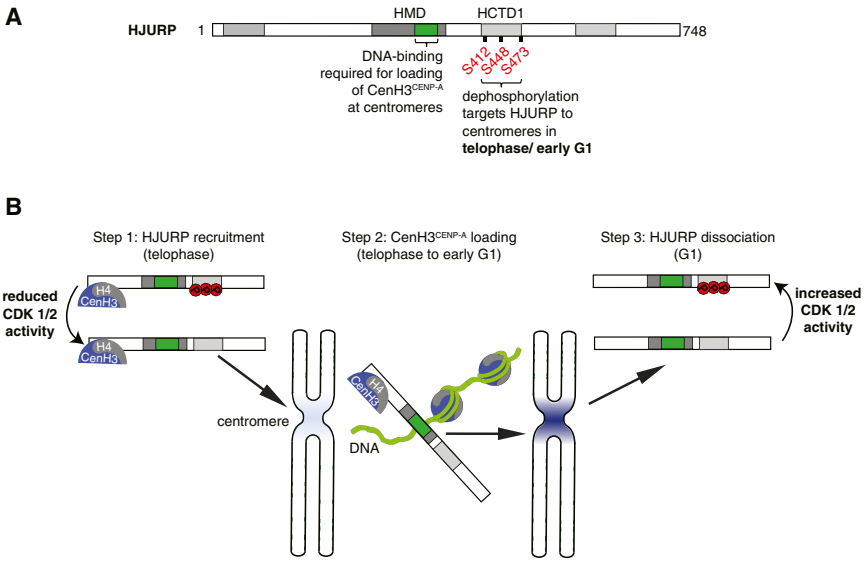

Figure 6. Model of CenH3^{CENP-A} Deposition by HJURP

(A) Functions of HJURP domains. DNA binding is indicated in green, and phosphorylation is in red.

(B) Model of the three-step mechanism of the CenH3^{CENP-A} chaperone function of HJURP at centromeres. In Step 1, HJURP is dephosphorylated in the HCTD1, which leads to its recruitment to centromeres in telophase/early G1, concomitant with reduced CDK1/CDK2 activity. In Step 2, HJURP loads CenH3^{CENP-A} at centromeres between telophase/early G1. It is actively involved in this process through its DNA-binding domain. In Step 3, HJURP is phosphorylated in the HCTD1, leading to a dissociation from centromeres, concomitant with increased CDK1/CDK2 activity.

interaction with DNA between telophase and early G1. This leads to an increase of CenH3^{CENP-A} at centromeres. In step 3, increased CDK activity leads to HJURP phosphorylation, which causes a dissociation of HJURP from centromeres where CenH3^{CENP-A} has been deposited.

Interestingly, the premature recruitment of Ala^{412,448,473} to centromeres results in CenH3^{CENP-A} loading in a subset of cells in G2, but not in S, whereas treatment with CDK inhibitors causes deposition in G2 and S. Thus, it is possible that during CenH3^{CENP-A} loading, HJURP may act in concert with (an)other CDK-responding factor(s) recruited in G2/M such as Mis18BP or Mis18β (Silva et al., 2012; Wang et al., 2014). Although we highlight here a temporal control for the loading CenH3^{CENP-A}, this control shows plasticity in different species and possibly during development. This is exemplified in flies with the timing of CenH3^{CID} deposition, which is altered in meiosis, when loading occurs during premeiotic G2, prophase I, and the spermatid stage in males and over a period of days during prophase I in females (Dunleavy et al., 2012; Raychaudhuri et al., 2012). In *C. elegans*, which have holocentromeres, an extreme situation has been reported. Unlike in vertebrates and flies, CenH3^{HCP-3} is lost in meiosis (Gassmann et al., 2012; Monen et al., 2005), and both oocyte meiotic divisions proceeded normally and recruited kinetochore proteins in the absence of CenH3^{HCP-3}. Surprisingly, a specific CenH3^{HCP-3}-loading factor has not yet been identified in this species because *C. elegans* have neither HJURP nor CAL1. Thus, the loading mechanism of CenH3 in a developmental context in other model organisms certainly illustrates an important plasticity. Dissecting this further might shed more light on the mechanisms of CenH3 recruitment and loading by its dedicated chaperone, such as CAL1 or HJURP.

A recent report proposed that Mis18β interacts with HJURP to recruit it to the centromere (Wang et al., 2014). Another recent study reported an interaction between HJURP and And-1, a protein required for CenH3^{CENP-A} incorporation at centromeres (Jaramillo-Lambert et al., 2013). In addition, CENP-C (Dambacher et al., 2012; Moree et al., 2011), CENP-N (Carroll et al., 2009), CENP-H/I (Okada et al., 2006), and Mis18 (Dambacher et al., 2012; Wang et al., 2014) are all required for CenH3^{CENP-A} deposition at centromeres in telophase/early G1. The presence of various other factors in the HJURP complex, including RbAp46/48 and Npm1, likely participates in these dynamics (Dunleavy et al., 2009). Future studies should address if and how these factors are involved in the mechanism of centromeric HJURP recruitment and/or the HJURP-mediated loading mechanism.

The different effects of the nonphosphorylatable mutant Ala^{412,448,473} and the DNA-binding mutant Δ285–321 on the cell cycle and on cell proliferation highlight the difference of the functionality of the HMD and the HCTD1 in HJURP localization to centromeres and CenH3^{CENP-A} loading, respectively. Taken together, our finding of a conserved DNA-binding region in the HMD of HJURP and its requirement for the loading of CenH3^{CENP-A} at centromeres provide insight into an active role for HJURP in the CenH3^{CENP-A}-loading mechanism. Given the preference of HJURP to interact with noncanonical DNA structures, in particular Holliday Junctions (Kato et al., 2007), this contribution to the loading mechanism might be mediated through structural changes of centromeric DNA. Interestingly, the HMD, including the newly identified DNA-binding domain, does not show a particular sequence conservation with other known DNA-binding proteins (Sanchez-Pulido et al., 2009). Therefore, future studies involving structural analyses of the HMD and how it interacts with DNA will be required to look into this issue in more detail. Currently, histone chaperones are

(B) Top: experimental scheme and western blot showing the expression of Ala^{412,448,473} and endogenous HJURP with siRNA treatment in the corresponding cell-cycle phases. Bottom view shows images of SNAP-CenH3^{CENP-A} U2OS cells transfected with the Ala^{412,448,473} mutant. Loading of TMR-star CenH3^{CENP-A} was observed in G2, and not in mid or late S. Scale bar, 5 μm. The bar chart represents percentages of Ala^{412,448,473}-transfected TMR-star-positive cells in mid-S, late S, and G2. Average of three independent experiments is shown. Error bars, SD.
See also Figure S6.

regarded as escort factors for their designated histone variants (reviewed in De Koning et al., 2007). We find that the functionality of HJURP as an active mechanistic participant in CenH3^{CENP-A} loading through its DNA-binding domain is distinct from a simple targeting role. A previous report showed that HIRA can interact with naked DNA, but this property is not common to all chaperones (Ray-Gallet et al., 2011). This raises the question as to whether other histone chaperones may also have similar additional roles in the histone-loading process. Thus, dissecting their loading mechanisms will be an interesting avenue for future research.

EXPERIMENTAL PROCEDURES

Cell Synchronization and Drugs

For synchronization in M and early G1, we incubated cells for 16 hr with nocodazole (Sigma-Aldrich) at 100 ng/ml. We subsequently washed the cells 2× with PBS and collected them (M phase/FACS) or plated them on collagen/fibronectin-coated coverslips (Sigma-Aldrich) or in culture dishes. We incubated them for 1 hr (early G1 for FACS) or 2 hr (early G1 for microscopy). For synchronization in G2 or S, we used a single thymidine block: we added thymidine (Sigma-Aldrich) to the cells (4 mM) and incubated them for 18 hr. Cells were washed 2× with PBS and 1× with medium and incubated in the presence of deoxycytidine (Sigma-Aldrich; 0.5 μM). We incubated cells with Roscovitine at 100 μM (Sigma-Aldrich) and Purvalanol A at 24 μM (Sigma-Aldrich) for 2 hr prior to fixation as indicated.

Transfection and siRNA

We transfected siRNAs and plasmids with jetPrime (Polyplus) according to the manufacturer's protocol. In a typical experiment, 24%–36% of cells were transfected with GFP-HJURP or the mutants. The siRNA sequences were ordered from MWG Eurofins and were as follows: siHJ, 5′-GAG-AUA-ACC-UCG-AGU-UCU-UTT-3′; and siLuc (control), 5′-CGU-ACG-CGG-AAU-ACU-UCG-A-3′.

Fluorescent Labeling for Microscopy

We performed pre-extraction of cells prior to fixation for 5 min with 0.5% Triton X-100 in CSK buffer as described by Martini et al. (1998) and fixed cells in 2% paraformaldehyde for 20 min. We blocked cells with BSA (5% in PBS, 0.1% Tween 20) before incubation with 1ry and 2ry antibodies and DAPI staining. For in vivo labeling of SNAP-tagged CenH3^{CENP-A}, we used the SNAP-labeling protocol as described by Jansen et al. (2007) and Ray-Gallet et al. (2011). We added 10 mM of SNAP-Cell Block (New England Biolabs) to cell medium at 37°C for 30 min to quench SNAP-tag activity (Q) and 2 mM SNAP-Cell TMR-Star (New England Biolabs) for 20 min for pulse labeling (P). We washed the cells 2× with PBS, reincubated them in medium for 10 min, and washed the cells 2× with PBS. For the chase (C), we incubated the cells for the indicated length of time. After in vivo labeling, the cells were processed for immunostaining. Synchronization with nocodazole or thymidine was incorporated into this protocol. For EdU labeling, we used the Click-iT EdU Alexa kit (Life Technologies) according to the manufacturer's instructions. To enhance GFP signals, we used the GFP-Trap booster (ChromoTek) at a dilution of 1:200, which was used prior to click chemistry in case of EdU labeling.

Pull-Down Studies

We produced GST-HJURP recombinant protein as described by Dunleavy et al. (2009) and obtained bead-linked plasmid DNA (PUC19) as described (Mello et al., 2004; Ray-Gallet et al., 2011). Mock beads or DNA beads were blocked with BSA (1 mg/ml) and incubated 1 hr at 30°C with 100 μg U2OS salt-extractable extracts or 100 ng recombinant proteins in buffer containing 10 mM HEPES (pH 7.8), 2 mM $MgCl_2$, 1 mM $CaCl_2$, 0.5 mM EGTA, 100 mM NaCl, 0.1% NP40, and 8% glycerol in a final volume of 50 μl. Then, the beads were washed 3× in the presence of 300 mM NaCl and 0.5% NP40. We analyzed bound proteins by western blot. We pulled down GFP-HJURP using GFP-Trap (ChromoTek) according to the manufacturer's protocol.

Antibodies

We used the following primary antibodies for western blotting: rabbit anti-HJURP (Sigma-Aldrich; #HPA008436, 1:500); rabbit anti-GFP (#A-P-R#06, in-house platform of Institut Curie, 1:1,000); anti-α-tubulin (Sigma-Aldrich; #T9026, 1:2,000); anti-Cabin1 (Abcam; #ab76600, 1:1,000); anti-HIRA (Active Motif; #WC119.2H11, 1:200); anti-Npm1 (Abcam; #ab15440, 1:1,000); anti-CenH3^{Cenp-A} (Cell Signaling Technology; #2186, 1:500); anti-RbAp48 (Abcam; ab1765, 1:1,000); anti-Caf-1 p150 (Abcam; #7655, 1:1,000); anti-CAF-1 p60 (Abcam; #ab8133, 1:1,000); and anti-GST (Abcam; ab9085, 1:500). The H3S10P antibody was a gift from N. Nozaki (Japan). We used the following secondary antibodies for immunofluorescence: anti-CREST = ACA (Fitzgerald Industries/Interchim; #90C-CS1058, 1:1,000); anti-Aurora B (BD Transduction Laboratories; #611082, 1:2,000); and anti-CENP-B (Abcam; #ab25734, 1:500). For immunofluorescence, we used Alexa 488-, Alexa 594-, Alexa 647-, or Cy5-coupled antibodies (Molecular Probes).

MS Analyses

Samples were analyzed using a LTQ Orbitrap XL mass spectrometer (Thermo Scientific) coupled to a nano-liquid chromatography system (UltiMate 3000; Dionex). Details of the separation, MS parameters, and label-free quantification are described in Supplemental Experimental Procedures.

SUPPLEMENTAL INFORMATION

Supplemental Information includes Supplemental Experimental Procedures and six figures and can be found with this article online at http://dx.doi.org/10.1016/j.celrep.2014.06.002.

ACKNOWLEDGMENTS

We thank Sylvain Cantaloube and Patricia Le Baccon for help with image analyses. We thank Dominique Ray-Gallet, Jean-Pierre Quivy, Christèle Maison, Lisa Prendergast, Isabelle Vassias, Zachary Gurard-Levin, and Hiroaki Tachiwana for discussion and careful proofreading. We thank Isabelle Vassias and Dan Filipescu for help with the production of recombinant protein. We thank Marie Curie/Nucleosome 4D and La Fondation pour la recherche médicale for postdoc fellowships (to S.M.). This work was supported by la Ligue Nationale contre le Cancer (Equipe labellisée Ligue), the European Commission Network of Excellence EpiGeneSys (HEALTH-F4-2010-257082), ERC Advanced Grant 2009-AdG_20090506 "Eccentric," the European Commission large-scale integrating project FP7_HEALTH-2010-259743 "MODHEP," ANR "ChromaTin" ANR-10-BLAN-1326-03, ANR-11-LABX-0044_DEEP, and ANR-10-IDEX-0001-02 PSL*, ANR "CHAPINHIB" ANR-12-BSV5-0022-02, and Aviesan-ITMO cancer project "Epigenomics of breast cancer."

Received: April 8, 2014
Revised: May 21, 2014
Accepted: June 1, 2014
Published: July 3, 2014

REFERENCES

Allshire, R.C., and Karpen, G.H. (2008). Epigenetic regulation of centromeric chromatin: old dogs, new tricks? Nat. Rev. Genet. *9*, 923–937.

Arellano, M., and Moreno, S. (1997). Regulation of CDK/cyclin complexes during the cell cycle. Int. J. Biochem. Cell Biol. *29*, 559–573.

Barnhart, M.C., Kuich, P.H., Stellfox, M.E., Ward, J.A., Bassett, E.A., Black, B.E., and Foltz, D.R. (2011). HJURP is a CENP-A chromatin assembly factor sufficient to form a functional de novo kinetochore. J. Cell Biol. *194*, 229–243.

Bassett, E.A., DeNizio, J., Barnhart-Dailey, M.C., Panchenko, T., Sekulic, N., Rogers, D.J., Foltz, D.R., and Black, B.E. (2012). HJURP uses distinct CENP-A surfaces to recognize and to stabilize CENP-A/histone H4 for centromere assembly. Dev. Cell *22*, 749–762.

Black, B.E., and Bassett, E.A. (2008). The histone variant CENP-A and centromere specification. Curr. Opin. Cell Biol. *20*, 91–100.

Boyarchuk, E., Montes de Oca, R., and Almouzni, G. (2011). Cell cycle dynamics of histone variants at the centromere, a model for chromosomal landmarks. Curr. Opin. Cell Biol. *23*, 266–276.

Carroll, C.W., Silva, M.C., Godek, K.M., Jansen, L.E., and Straight, A.F. (2009). Centromere assembly requires the direct recognition of CENP-A nucleosomes by CENP-N. Nat. Cell Biol. *11*, 896–902.

Cheeseman, I.M., Drubin, D.G., and Barnes, G. (2002). Simple centromere, complex kinetochore: linking spindle microtubules and centromeric DNA in budding yeast. J. Cell Biol. *157*, 199–203.

Chen, C.C., Dechassa, M.L., Bettini, E., Ledoux, M.B., Belisario, C., Heun, P., Luger, K., and Mellone, B.G. (2014). CAL1 is the *Drosophila* CENP-A assembly factor. J. Cell Biol. *204*, 313–329.

Choi, E.S., Strålfors, A., Castillo, A.G., Durand-Dubief, M., Ekwall, K., and Allshire, R.C. (2011). Identification of noncoding transcripts from within CENP-A chromatin at fission yeast centromeres. J. Biol. Chem. *286*, 23600–23607.

Cleveland, D.W., Mao, Y., and Sullivan, K.F. (2003). Centromeres and kinetochores: from epigenetics to mitotic checkpoint signaling. Cell *112*, 407–421.

Dambacher, S., Deng, W., Hahn, M., Sadic, D., Fröhlich, J., Nuber, A., Hoischen, C., Diekmann, S., Leonhardt, H., and Schotta, G. (2012). CENP-C facilitates the recruitment of M18BP1 to centromeric chromatin. Nucleus *3*, 101–110.

De Koning, L., Corpet, A., Haber, J.E., and Almouzni, G. (2007). Histone chaperones: an escort network regulating histone traffic. Nat. Struct. Mol. Biol. *14*, 997–1007.

Dephoure, N., Zhou, C., Villén, J., Beausoleil, S.A., Bakalarski, C.E., Elledge, S.J., and Gygi, S.P. (2008). A quantitative atlas of mitotic phosphorylation. Proc. Natl. Acad. Sci. USA *105*, 10762–10767.

Dunleavy, E.M., Roche, D., Tagami, H., Lacoste, N., Ray-Gallet, D., Nakamura, Y., Daigo, Y., Nakatani, Y., and Almouzni-Pettinotti, G. (2009). HJURP is a cell-cycle-dependent maintenance and deposition factor of CENP-A at centromeres. Cell *137*, 485–497.

Dunleavy, E.M., Almouzni, G., and Karpen, G.H. (2011). H3.3 is deposited at centromeres in S phase as a placeholder for newly assembled CENP-A in G_1 phase. Nucleus *2*, 146–157.

Dunleavy, E.M., Beier, N.L., Gorgescu, W., Tang, J., Costes, S.V., and Karpen, G.H. (2012). The cell cycle timing of centromeric chromatin assembly in *Drosophila* meiosis is distinct from mitosis yet requires CAL1 and CENP-C. PLoS Biol. *10*, e1001460.

Earnshaw, W.C., and Rothfield, N. (1985). Identification of a family of human centromere proteins using autoimmune sera from patients with scleroderma. Chromosoma *91*, 313–321.

Earnshaw, W.C., and Cleveland, D.W. (2013). CENP-A and the CENP nomenclature: response to Talbert and Henikoff. Trends Genet. *29*, 500–502.

Earnshaw, W.C., Allshire, R.C., Black, B.E., Bloom, K., Brinkley, B.R., Brown, W., Cheeseman, I.M., Choo, K.H., Copenhaver, G.P., Deluca, J.G., et al. (2013). Esperanto for histones: CENP-A, not CenH3, is the centromeric histone H3 variant. Chromosome Res. *21*, 101–106.

Fachinetti, D., Folco, H.D., Nechemia-Arbely, Y., Valente, L.P., Nguyen, K., Wong, A.J., Zhu, Q., Holland, A.J., Desai, A., Jansen, L.E., and Cleveland, D.W. (2013). A two-step mechanism for epigenetic specification of centromere identity and function. Nat. Cell Biol. *15*, 1056–1066.

Flemming, W. (1882). Zellsubstanz (Leipzig: Kern und Zelltheilung. FCW Vogel).

Foltz, D.R., Jansen, L.E., Bailey, A.O., Yates, J.R., 3rd, Bassett, E.A., Wood, S., Black, B.E., and Cleveland, D.W. (2009). Centromere-specific assembly of CENP-a nucleosomes is mediated by HJURP. Cell *137*, 472–484.

Fujita, Y., Hayashi, T., Kiyomitsu, T., Toyoda, Y., Kokubu, A., Obuse, C., and Yanagida, M. (2007). Priming of centromere for CENP-A recruitment by human hMis18alpha, hMis18beta, and M18BP1. Dev. Cell *12*, 17–30.

Gascoigne, K.E., Takeuchi, K., Suzuki, A., Hori, T., Fukagawa, T., and Cheeseman, I.M. (2011). Induced ectopic kinetochore assembly bypasses the requirement for CENP-A nucleosomes. Cell *145*, 410–422.

Gassmann, R., Rechtsteiner, A., Yuen, K.W., Muroyama, A., Egelhofer, T., Gaydos, L., Barron, F., Maddox, P., Essex, A., Monen, J., et al. (2012). An inverse relationship to germline transcription defines centromeric chromatin in *C. elegans*. Nature *484*, 534–537.

Hu, H., Liu, Y., Wang, M., Fang, J., Huang, H., Yang, N., Li, Y., Wang, J., Yao, X., Shi, Y., et al. (2011). Structure of a CENP-A-histone H4 heterodimer in complex with chaperone HJURP. Genes Dev. *25*, 901–906.

Hwang, S., Gou, Z., and Kuznetsov, I.B. (2007). DP-Bind: a web server for sequence-based prediction of DNA-binding residues in DNA-binding proteins. Bioinformatics *23*, 634–636.

Jansen, L.E., Black, B.E., Foltz, D.R., and Cleveland, D.W. (2007). Propagation of centromeric chromatin requires exit from mitosis. J. Cell Biol. *176*, 795–805.

Jaramillo-Lambert, A., Hao, J., Xiao, H., Li, Y., Han, Z., and Zhu, W. (2013). Acidic nucleoplasmic DNA-binding protein (And-1) controls chromosome congression by regulating the assembly of CENP-A at centromeres. J. Biol. Chem. *288*, 1480–1488.

Kato, T., Sato, N., Hayama, S., Yamabuki, T., Ito, T., Miyamoto, M., Kondo, S., Nakamura, Y., and Daigo, Y. (2007). Activation of Holliday junction recognizing protein involved in the chromosomal stability and immortality of cancer cells. Cancer Res. *67*, 8544–8553.

Kuznetsov, I.B., Gou, Z., Li, R., and Hwang, S. (2006). Using evolutionary and structural information to predict DNA-binding sites on DNA-binding proteins. Proteins *64*, 19–27.

Lacoste, N., Woolfe, A., Tachiwana, H., Garea, A.V., Barth, T., Cantaloube, S., Kurumizaka, H., Imhof, A., and Almouzni, G. (2014). Mislocalization of the centromeric histone variant CenH3/CENP-A in human cells depends on the chaperone DAXX. Mol. Cell *53*, 631–644.

Marheineke, K., and Krude, T. (1998). Nucleosome assembly activity and intracellular localization of human CAF-1 changes during the cell division cycle. J. Biol. Chem. *273*, 15279–15286.

Martini, E., Roche, D.M., Marheineke, K., Verreault, A., and Almouzni, G. (1998). Recruitment of phosphorylated chromatin assembly factor 1 to chromatin after UV irradiation of human cells. J. Cell Biol. *143*, 563–575.

Mello, J.A., Moggs, J.G., and Almouzni, G. (2004). Analysis of DNA repair and chromatin assembly in vitro using immobilized damaged DNA substrates. Methods Mol. Biol. *281*, 271–281.

Mellone, B.G., Grive, K.J., Shteyn, V., Bowers, S.R., Oderberg, I., and Karpen, G.H. (2011). Assembly of *Drosophila* centromeric chromatin proteins during mitosis. PLoS Genet. *7*, e1002068.

Mishra, P.K., Au, W.C., Choy, J.S., Kuich, P.H., Baker, R.E., Foltz, D.R., and Basrai, M.A. (2011). Misregulation of Scm3p/HJURP causes chromosome instability in *Saccharomyces cerevisiae* and human cells. PLoS Genet. *7*, e1002303.

Monen, J., Maddox, P.S., Hyndman, F., Oegema, K., and Desai, A. (2005). Differential role of CENP-A in the segregation of holocentric *C. elegans* chromosomes during meiosis and mitosis. Nat. Cell Biol. *7*, 1248–1255.

Moree, B., Meyer, C.B., Fuller, C.J., and Straight, A.F. (2011). CENP-C recruits M18BP1 to centromeres to promote CENP-A chromatin assembly. J. Cell Biol. *194*, 855–871.

Müller, S., and Almouzni, G. (2014). A network of players in H3 histone variant deposition and maintenance at centromeres. Biochim. Biophys. Acta *1839*, 241–250.

Okada, M., Cheeseman, I.M., Hori, T., Okawa, K., McLeod, I.X., Yates, J.R., 3rd, Desai, A., and Fukagawa, T. (2006). The CENP-H-I complex is required for the efficient incorporation of newly synthesized CENP-A into centromeres. Nat. Cell Biol. *8*, 446–457.

Pearson, C.G., Yeh, E., Gardner, M., Odde, D., Salmon, E.D., and Bloom, K. (2004). Stable kinetochore-microtubule attachment constrains centromere positioning in metaphase. Curr. Biol. *14*, 1962–1967.

Pidoux, A.L., Choi, E.S., Abbott, J.K., Liu, X., Kagansky, A., Castillo, A.G., Hamilton, G.L., Richardson, W., Rappsilber, J., He, X., and Allshire, R.C. (2009). Fission yeast Scm3: a CENP-A receptor required for integrity of subkinetochore chromatin. Mol. Cell *33*, 299–311.

Probst, A.V., Dunleavy, E., and Almouzni, G. (2009). Epigenetic inheritance during the cell cycle. Nat. Rev. Mol. Cell Biol. *10*, 192–206.

Raychaudhuri, N., Dubruille, R., Orsi, G.A., Bagheri, H.C., Loppin, B., and Lehner, C.F. (2012). Transgenerational propagation and quantitative maintenance of paternal centromeres depends on Cid/Cenp-A presence in *Drosophila* sperm. PLoS Biol. *10*, e1001434.

Ray-Gallet, D., Woolfe, A., Vassias, I., Pellentz, C., Lacoste, N., Puri, A., Schultz, D.C., Pchelintsev, N.A., Adams, P.D., Jansen, L.E., and Almouzni, G. (2011). Dynamics of histone H3 deposition in vivo reveal a nucleosome gap-filling mechanism for H3.3 to maintain chromatin integrity. Mol. Cell *44*, 928–941.

Sanchez-Pulido, L., Pidoux, A.L., Ponting, C.P., and Allshire, R.C. (2009). Common ancestry of the CENP-A chaperones Scm3 and HJURP. Cell *137*, 1173–1174.

Schuh, M., Lehner, C.F., and Heidmann, S. (2007). Incorporation of *Drosophila* CID/CENP-A and CENP-C into centromeres during early embryonic anaphase. Curr. Biol. *17*, 237–243.

Shivaraju, M., Camahort, R., Mattingly, M., and Gerton, J.L. (2011). Scm3 is a centromeric nucleosome assembly factor. J. Biol. Chem. *286*, 12016–12023.

Shuaib, M., Ouararhni, K., Dimitrov, S., and Hamiche, A. (2010). HJURP binds CENP-A via a highly conserved N-terminal domain and mediates its deposition at centromeres. Proc. Natl. Acad. Sci. USA *107*, 1349–1354.

Silva, M.C., Bodor, D.L., Stellfox, M.E., Martins, N.M., Hochegger, H., Foltz, D.R., and Jansen, L.E. (2012). Cdk activity couples epigenetic centromere inheritance to cell cycle progression. Dev. Cell *22*, 52–63.

Takayama, Y., Sato, H., Saitoh, S., Ogiyama, Y., Masuda, F., and Takahashi, K. (2008). Biphasic incorporation of centromeric histone CENP-A in fission yeast. Mol. Biol. Cell *19*, 682–690.

Talbert, P.B., and Henikoff, S. (2013). Phylogeny as the basis for naming histones. Trends Genet. *29*, 499–500.

Talbert, P.B., Ahmad, K., Almouzni, G., Ausio, J., Berger, F., Bhalla, P.L., Bonner, W.M., Cande, W.Z., Chadwick, B.P., Chan, S.W., et al. (2012). A unified phylogeny-based nomenclature for histone variants. Epigenetics Chromatin *5*, 7.

Wang, J., Liu, X., Dou, Z., Chen, L., Jiang, H., Fu, C., Fu, G., Liu, D., Zhang, J., Zhu, T., et al. (2014). Mitotic regulator Mis18beta interacts with and specifies the centromeric assembly of molecular chaperone holliday junction recognition protein (HJURP). J. Biol. Chem. *289*, 8326–8336.

Xiao, H., Mizuguchi, G., Wisniewski, J., Huang, Y., Wei, D., and Wu, C. (2011). Nonhistone Scm3 binds to AT-rich DNA to organize atypical centromeric nucleosome of budding yeast. Mol. Cell *43*, 369–380.

Zasadzińska, E., Barnhart-Dailey, M.C., Kuich, P.H., and Foltz, D.R. (2013). Dimerization of the CENP-A assembly factor HJURP is required for centromeric nucleosome deposition. EMBO J. *32*, 2113–2124.